Naunyn-Schmiedeberg's Archives of Pharmacology
https://doi.org/10.1007/s00210-019-01664-9

ORIGINAL ARTICLE

Acylated ghrelin prevents doxorubicin-induced cardiac intrinsic cell death and fibrosis in rats by restoring IL-6/JAK2/STAT3 signaling pathway and inhibition of STAT1

Ali A. Shati[1] · Attalla Farag El-kott[1,2]

Received: 14 February 2019 / Accepted: 2 May 2019

Abstract
This study investigated if JAK/STAT signaling pathway mediates doxorubicin (DOX)-induced cell death and fibrosis in left ventricles (LVs) of rats and examined if acylated ghrelin affords protection by modulating this pathway. Male rats (120 ± 5 g) were divided into 6 groups (10 rats each) as follows: control; control + AG (10 ng/kg, s.c.); DOX (an accumulative dose 15 mg/kg, i.p.); DOX + AG, DOX + AG + AG490, a JAK2 inhibitor (5 mg/kg, i.p.); and DOX + AG + [D-Lys3]-GHRP-6; an AG receptor antagonist (3.75 mg/kg, i.p.). All treatments were carried out for 35 days. In rats' LVs, DOX significantly impaired the systolic and diastolic functions, enhanced levels of ROS and MDA, reduced levels of GSH and Bcl-2, and increased mRNA and protein levels of collagen I/III and TGF-β and cleaved caspase-3. In addition, although DOX did not affect JAK1 or JAK2 activity, it significantly increased protein levels of IL-6, decreased STAT3 and p-STAT3 (Tyr701&Ser727), and increased STAT1 and p-STAT1 (Tyr701&Ser727) levels, with a concomitant decrease in ERK1/2 activity and an increase in P38 activity. However, without affecting IL-6 and JAK1/2, AG reversed all of the observed alterations with a significant increase in the levels and activities of JAK2. Similar effects of AG were also seen in control rats. Interestingly, all the beneficial effects afforded by AG were abolished by AG490 and AG + [D-Lys3]-GHRP-6. In conclusion, DOX-induced cardiac toxicity involves stimulation of IL-6, P38, and STAT1 signaling levels whereas the protective effect afforded by AG involves the activation of ERK1/2 and JAK2/STAT3 and inhibition of STAT1.

Keywords Ghrelin · Doxorubicin · JAK/STAT · IL-6 · Rats

Introduction

Doxorubicin (DOX)-induced cardiotoxicity is characterized by rhythmic deregulation, reduced left ventricular (LV) contractility, myocyte apoptosis, fibrosis, and ultimately, heart failure (HF) (Hong et al. 2017; Johnson and Singla 2018). Overproduction of reactive oxygen species (ROS), reduction in myocardial antioxidant potential, inhibition of nucleic acid and protein synthesis, mitochondria damage, inflammation, and apoptosis are the most common known mechanisms that are involved in DOX-induced cardiomyopathy (Wang et al. 2002; Riad et al. 2009; Mantawy et al. 2014; Wu et al. 2017). In spite of this, treatment options remain limited and may be explained by the incomplete understanding of the complexity of the interconnected molecular mechanisms involved.

The Janus kinase/signal transducer and activator of transcription (JAK/STAT) signal transduction pathway is a master signaling pathway that regulates cell survival, apoptosis, hypertrophy, and collagen synthesis in the heart of mammals and is activated in response to oxidative stress, inflammatory cytokines, and growth factors (Barry et al. 2007). JAK1, JAK2, STAT1, and STAT3 are the most prominent members found in the mammalian's heart (Booz et al. 2002; Hilfiker-Kleiner et al. 2004; Barry et al. 2007). While STAT1 is a pro-apoptotic and fibrotic transcription factor acting through activation of caspases, Fas/Fas ligand (FasL) axis, and p53, STAT3 is a survival factor that acts in an opposite way (Stephanou et al. 2000;

✉ Ali A. Shati
aalshati@kku.edu.sa

[1] Biology Department, College of Science, King Khalid University, Abha, Saudi Arabia

[2] Zoology Department, College of Science, Damanhour University, Damanhour, Egypt

Published online: 16 May 2019

Negoro et al. 2001; Wang et al. 2002; Harada et al. 2005; Barry et al. 2007; Scarabelli et al. 2009; Dai et al. 2013; Liu et al. 2018).

Until now, the contribution of the JAK/STAT pathway in DOX-induced cardiotoxicity is not completely understood and needs further investigation. However, the currently available studies may support the hypothesis that alterations in JAK/STAT signaling could have a significant role in the pathogenesis of DOX-induced cardiotoxicity. Indeed, mice with cardiac-specific deletion of STAT3 are more sensitive to DOX-induced cardiac inflammation and fibrosis (Jacoby et al. 2003). Also, mRNA of STAT-3 was significantly reduced in the heart of wild-type mice after 2 days of DOX treatment, and transgenic mice overexpressing STAT-3 were protected against DOX-induced cardiac damage and have a high survival rate (Kunisada et al. 2000). In addition, decreased levels of total STAT-3, p-STAT-3, JAK2, and p-JAK-2 and reduced number of STAT-3-positive cardiomyocytes were seen in the heart of patients with failing heart (Podewski et al. 2003). Due to a paucity of enough supporting evidence, the role of JAK/STAT signaling in the cardiomyocyte cell apoptosis after DOX treatment should be investigated more.

On the other hand, ghrelin, a hormone released mainly from gastric mucosa, has been recently given much interest as a potent cardioprotective hormone in both humans and animals (Baldanzi et al. 2002; Zhang et al. 2010). Ghrelin circulates in the bloodstream either as acylated ghrelin (AG) (5%) and desacyl-ghrelin (DAG) (95%). Both AG and DAG were shown to have cardioprotective effects (Chang et al. 2004a; Zhang et al. 2010; Pei et al. 2013).

By acting peripherally through the growth hormone secretagogue receptor-1a (GHSR1a), AG cardioprotection was shown in various animal models of cardiotoxicity, including ischemia/reperfusion injury (I/R), myocardial infarction (MI), HF, isoproterenol-induced injury, diabetic cardiomyopathy, and DOX-induced cardiotoxicity, and it was mediated at least, by improving contractility and cardiac output, vasodilation, boosting cardiac antioxidant potential, reducing infarct size, and inhibition of cardiac apoptosis and fibrosis (Bisi et al. 1999; Nagaya et al. 2001a, b, 2004; Frascarelli et al. 2003; Chang et al. 2004a, b; Pei et al. 2014; Yang et al. 2014; Pei et al. 2015; Eid et al. 2018). Confirmed molecular cardioprotective cardiovascular mechanisms afforded by AG include activation of survival pathways, such as ERK1/2, PI3K/Akt, cyclic adenosine monophosphate (cAMP)/protein kinase A (PKA), inhibition of angiotensin II, and inflammation (Xu et al. 2007, 2008; Huang et al. 2009; Kui et al. 2009; Xiang et al. 2011; Pei et al. 2014; Yang et al. 2014). Interestingly, in a very well-designed study, AG prevented apoptosis in the LV of MI-induced rats by inhibition of STAT1 and activation of STAT3 (Eid et al. 2018).

Regarding DOX-induced cardiotoxicity, AG inhibited DOX-induced ROS and cell apoptosis and increased cardiomyocyte size in the hearts of mice by inhibiting excessive autophagy through inhibition of AMPK and stimulating p38-MAPK and mTOR (Wang et al. 2014). In H9c2, AG prevented DOX-induced cell apoptosis by activation of ERK and Akt (Baldanzi et al. 2002). Also, dietary ghrelin-containing Salmon stomach extra improved LV function and reduced collagen deposition in DOX-treated mice (Kihara et al. 2016).

Given the above-mentioned pieces of evidence, in this study, we hypothesized that DOX induces cardiac apoptosis and fibrosis by inhibition of STAT3 and activation of STAT1 and that concomitant administration of AG is able to mitigate this by stimulation of STAT3 signaling and inhibition of STAT1. In addition, we investigated the regulation mechanisms afforded by DOX and AG on STAT1 and STAT3, including their effects on ROS generation as well as on the activities of JAK1/2, ERK1/2, and P38 MAPK.

Materials and methods

Chemicals and antibodies

Synthetic AG (Cat. No. G8903), tyrphostin AG490 (Cat. No. 133550-30-8), [D-Lys3]-GHRP-6 (Cat. No. G4535), and doxorubicin hydrochloride (DOX) (Cat. No. D1515) were purchased from Sigma-Aldrich, UK. Antibodies against JAK1 (Cat. No. 3332, 130 kDa), p-JAK 1 ($Tyr^{1034/1035}$) (Cat. No. 3331, 130 kDa), p-JAK2 ($Tyr^{1007/1008}$) (Cat. No. 3771, 125 kDa), p-STAT3 (Ser^{727}) (Cat. No. 9134, 86 kDa), STAT 1 (Cat. No. 9172, 84/91 kDa), p-Smad3 (Ser423/425) (Cat. No. 9520, 52 kDa), p-ERK1/2 (Thr202/Tyr204) (Cat. No. 4370, 44/42 kDa, CST), cleaved caspase-3 (Cat. No. 9661, 17/19 kDa), and β-actin (Cat. No. 4970, 45 kDa, SCT) were purchased from Cell Signaling Technology, USA. Antibodies against JAK2 (Cat. No. sc-390539, 128 kDa), STAT3 (Cat. No. sc-8019, 86/91 kDa), p-STAT1 (Ser^{727}) (Cat. No. sc-51700, 48/91 kDa), TGFβ-1 (Cat. No. sc-130348, 13–25 kDa), IL-6Rα1 (Cat. No. sc-374259, 80 kDa), IL-6 (Cat. No. sc-28343, 21 kDa), Bax (Cat. No. 7480, 23 kDa), and Bcl-2 (Cat. No. 7382, 26 kDa) were purchased from Santa Cruz Biotechnology, USA.

Animals and ethical statement

Adult male healthy Wistar rats (120 ± 5 g, 7 weeks old) were obtained from and maintained in the animal facility unit at King Khalid University (KKU) in Abha, Saudi Arabia. All rats lived under controlled conditions (temperature = 22 ± 1 °C, humidity = 60%, and a 12-h light/dark cycle). During the adaptation period of one week and the experimental

procedure, all rats were fed control chow and had free access to drinking water. All procedures performed in this study, including animal handling, surgery, sampling, and blood and tissue collection, were approved by the Ethical Committee for the use and care of laboratory animals at KKU and followed the guidelines for the use and care of laboratory animals established by the US National Institutes of Health (NIH publication no. 85-23, revised 1996).

Experimental design

The animals were assigned randomly into the following 6 groups ($n = 10$, each): (1) a control-untreated group administered with normal saline (0.1 ml) as vehicle (s.c.); (2) an AG-treated group administered an equivalent dose of synthetic rat's AG (10 ng/kg, s.c.); (3) a DOX-treated group that received DOX (an accumulative dose of 15 mg/kg, i.p.) over a period of 2 weeks (2.5 mg/kg, 6 doses), and co-received normal saline as vehicle (0.1 ml, s.c.); (4) DOX + AG-treated rats administered DOX as mentioned in group 3 and received a concomitant dose of AG (10 ng/kg, s.c.); (5) DOX + AG + AG490 treated as in group 4 and received a concomitant dose of tyrphostin AG490, a JAK2 inhibitor (5 mg/kg, i.p.); and (6) DOX + AG + [D-Lys3]-GHRP-6 treated as in group 4 and received a concomitant dose of [D-Lys3]-GHRP-6, an AG receptor (GHSR1a) antagonist (3.75 mg/kg, i.p.). AG490 and [D-Lys3]-GHRP-6 in the treated groups were started 4 h before DOX and AG administration and continued on a daily basis.

All treatments were conducted on a daily basis for 35 days. The dose and preparation of DOX were adopted from the study of Lou et al. (2005) who showed the development of HF in the animals after 3 weeks of the last DOX dose. The dose and preparation of AG were based on other studies (Li et al. 2013; Işeri et al. 2008) that have shown such dose results in a physiological increase in circulatory AG levels and is protective against tissue-induced oxidative stress and inflammation without affecting food intake. In addition, this has been confirmed in our preliminary experiments and confirmed by the results of this study (shown in the subsequent texts). The doses, preparation, and routes of administration of AG490 and [D-Lys3]-GHRP-6 were based on studies of Eid et al. (2018) and Pei et al. (2015), respectively, who have shown that such doses lead to complete inhibition of JAK2 and AG signaling in the heart of animals.

Hemodynamic measurements

Between days 36 and 37, hemodynamic parameters were recorded in all rats (5 randomly selected rats/group/day) in an open-heart surgery as previously established in our labs (Eid et al. 2018) using a pre-calibrated SPR-320 pressure catheter connected to PowerLab data acquisition system (model no. 4/26, AD Instruments Ltd., Australia). In brief, the rats were anesthetized with (1% sodium pentobarbital solution, 50 mg/kg) and placed on a heated pad. After successful ventilation, their chest was opened and the Millar catheter was directly stabbed into their LVs. The signal was recorded for 30 min and analyzed using LabChart software (V8, AD Instruments Ltd., Australia). Parameters calculated were LV systolic pressure (LVSP), LV end-diastolic pressure (LVEDP), maximal rate of increase in LV pressure ($LVdP/dt_{max}$), and maximal rate of decrease in LV pressure ($LVdP/dt_{min}$).

Serum and tissue collection

At the end of the hemodynamics recording, 2 ml of blood samples was collected directly from the carotid artery into EDTA tubes, centrifuged to collect plasma which was used freshly to measure levels of circulatory AG or were stored for further biochemical analysis. Also, LVs were directly isolated and rapidly washed with ice-cold phosphate-buffered saline (PBS, pH = 7.4). Then, they were cut on ice into smaller pieces, some of which were frozen at − 80 °C for biochemical and molecular analysis studies or were processed for electron microscopy studies.

Biochemical analysis in the serum

Plasma levels of brain natriuretic peptide (BNP) and creatine kinase-MB (CK-MB) were measured using commercial rat's ELISA kits (Cat. No ab108816, Abcam, UK, and Cat. No. E4608, BioVision, USA, respectively). Plasma levels of AG were measured in the plasma samples within three days after blood collection using special rat's ELISA kit (Cat. No. A05117, SPI Bio, France), which is provided with reagents to prevent AG degradation. All procedures were carried out in duplicate in accordance with the manufacturer's instruction.

Preparation of total cell homogenates

To prepare total homogenates, frozen LVs were homogenized in 0.5 ml RIPA buffer containing 0.1% SDS, 1.0% NP-40, or Triton X-100; 150 mM sodium chloride, 0.5% sodium deoxycholate; and 50 mM Tris (pH 8.0) plus protease inhibitors (Cat. No. P8340, Sigma-Aldrich, St. Louis, MO, USA). The total cell homogenates were centrifuged at 600*g* for 10 min to remove unbroken cells, nuclei, and excess cytoskeletal, and their supernatants were collected and stored at − 80 °C for further analysis.

Protein levels in the collected supernatants were measured in duplicate using a Pierce BCA Protein Assay Kit (Cat. No. 23225, Thermo Fisher Scientific).

Biochemical measurements in LVs

Total levels of ROS were measured in the LV homogenates of all rats using an in vitro assay kit (OxiSelect, Cat. No. STA-347, Cell Biolabs, Inc., San Diego, CA). Levels of reduced glutathione (GSH), malondialdehyde (MDA), and IL-6 in the LV homogenates of all rats were measured using assay kits (Cat. No. ab156681, Abcam, Cambridge, UK; Cat. No. NWK-MDA01, NWLSS, USA; and Cat No. ELR-IL6-001, RayBio, MO, USA, respectively). Total collagen contents in LV homogenates of all rats were measured using a colorimetric assay kit (ab222942, Abcam, Cambridge, UK). All procedures were carried out in duplicate in accordance with the manufacturer's instruction.

Quantitative real-time PCR in LVs

Primers used to study mRNA levels of collagen I, collagen III, TGF-β1, and β-actin are shown in Table 1. Total RNA was extracted from frozen LVs (20 mg) using an RNeasy Mini Kit (Cat. No. 74104, Qiagen, Victoria, Australia), and their purities were determined by having the absorbance 260/280 (Nanodrop spectrophotometer). Single-stranded cDNA was synthesized using SuperScript II reverse transcriptase kit using oligo(dT) primers (Cat. No. 18064014, Thermo Fisher, MA, USA). q-PCR reactions were performed in duplicate using a CFX96 real-time PCR system (Bio-Rad, CA, USA) using SofastEvagreenSupermix (Cat. No. 172-5200, BioRad, Montreal, Canada). As a positive control, template DNA was omitted from each palate. All measurements were performed in accordance with the manufacturer's instructions.

Western blotting analysis

Protein samples (40 μg) form all rats of various groups were resolved on 8–12% SDS polyacrylamide gel electrophoresis (SDS-PAGE), transferred to nitrocellulose membrane, and incubated, at room temperature for 2 h with shaking, with the primary. Membranes were then washed and incubated with the corresponding secondary antibodies at room temperature for another 2 h on a shaker. Membranes were stripped up to 5 times in which the detection of phosphorylated forms was done first and the loading control is the last. Antigen–antibody interactions were visualized using enhanced chemiluminescence detection reagent (Pierce ECL reagents, Thermo Fisher, Piscataway, NJ, USA) and quantified using C-DiGit blot scanner and software (LI-COR, USA). All proteins were normalized with the loading control, and activation ratio of some proteins was calculated as relative expression of the phosphorylated protein to the loading dye over the relative expression of its total protein levels to the loading dye.

Transmission electron microscope procedure

Cardiac tissues from the LVs of all groups of rats were cut freshly into 2–3 mm^2 sections and immediately fixed by immersion in 2.5% glutaraldehyde with 0.1 M sodium cacodylate buffer (pH 7.4) at 4 °C for 2–3 h. Specimens were post-fixed in 1% osmium tetroxide with the same buffer (0.1 M sodium cacodylate buffer, pH 7.4) for 1–2 h, dehydrated in ascending series of ethanol, and embedded in Spur's resin. Semi-thin sections (0.5–1 μm) were discolored with toluidine blue. Ultrathin sections were stained with both uranyl acetate and lead citrate stains and examined in a transmission electron microscope (JEM-1011, Jeol Co., Japan, at 80 Kv) (Eid et al. 2018). At least three specimens/group were investigated.

Masson's trichrome staining

Paraffin-embedded sections (4 μm in thickness) were stained with Masson's trichrome as previously described (Masson 1929). Photos were taken using Axiovert 200 M microscope and a digital camera (Model No. D30, Hitachi). At least three slides/group were investigated.

Caspase-3 immunohistochemistry

Immunohistochemistry for caspase-3 in the cardiac tissue was performed on paraffin-embedded sections (4 μm) according to

Table 1 Primers and conditions used in PCR reactions

Target	Accession no	Primer sequence (5′ to 3′)	(bp)
Collagen I	NM_053304.1	F: TTCACCTACAGCACGCTTGT R: TTGGGATGGAGGGAGTTTAC	196
Collagen III	NM_032085.1	F: GTTGAATATCAAACACGCAAGGC R: GTCACTTTCACTGGTTGACGA	201
TGF-β1	NM_021578.2	F: TAATGGTGGACCGCAACAACG R: GGCACTGCTTCCCGAATGTCT	100
β-Actin	NM_031144.3	F: AGACCTTCAACACCCCAG R: CACGATTTCCCTCTCAGC	254

the method described by Bressenot et al. (2009) with some modification. Sections were first dewaxed, rehydrated, and exposed to antigen retrieval (in 10 mM citrate buffer, pH 6) for 10 min boiling in a microwave followed by a 2-h cool-down. Then, the sections were washed twice in PBST (10 min/each), and the endogenous peroxidase activity was blocked with 3% H_2O_2 prepared in distilled water (Sigma, UK) for 30 min at room temperature. The sections were then washed again with PBST and incubated with 4% (*v*/*v*) goat serum (DakoCytomation; Trappes, France) at room temperature for another 20 min to block the non-specific binding sites. Excess serum was removed by blotting, and the sections were incubated with the primary anti-rabbit active caspase-3 antibody (Cat. No.9661, Cell Signalling Technology, Danvers, MA), prepared for 16 h at 4 °C in a moisture box. The sections were then washed twice in PBST (10 min/each) and incubated for 1 h at room temperature with biotinylated goat anti-rabbit antibody (DakoCytomation; Trappes, France) at a dilution of 1:200. Antibodies were diluted in 0.1 M PBS (pH = 7.4) buffer containing 0.3% (m/v) BSA, 20% (*v*/*v*) glycerol, 0.06% (m/v) n-ethyl-maleimide, and 0.1% (m/v) sodium azide. After that, the slides were washed twice with PBST (5 min/each) and incubated at room temperature for 30 min with 0.5% (*v*/*v*) streptavidin (DakoCytomation, Ely, UK) prepared in PBST. The slides were washed again and then treated with DAB for 10 min at room temperature, washed in tap water, and counterstained in hematoxylin. Photos were taken using Axiovert 200 M microscope and a digital camera (Model No. D30, Hitachi).

Statistical analysis

Statistical analysis for all measured parameters was done using GraphPad Prism statistical software package (version 6). Differences among the experimental groups were assessed by one-way ANOVA and followed by Tukey's test. Data were presented as mean ± SD. Values will be considered significantly different when $P < 0.05$.

Results

Administration of AG enhances plasma levels of AG in both control and DOX-treated rats

DOX significantly lowered circulatory plasma levels of AG in the treated rats as compared to control rats (Table 1). Administration of AG to control or DOX-treated rats significantly increased circulatory plasma level of AG by 51 and 71%, respectively (Table 1). Co-administration of AG490 (a JAK2 inhibitor) or +[D-Lys3]-GHRP-6 (a GHSR1a antagonist) to DOX + AG-treated rats did not affect plasma levels of AG, and its plasma levels in these groups of treated rats remained not statistically significant as compared to those measured in the plasma of DOX + AG-treated rats and were not significantly different when compared to each other (Table 1).

Administration of AG improves cardiac function in both control and DOX-treated rats

There was no significant change in heart rate (HR) among all experimental groups of all treatments (Table 1). Values of LVSP, dp/dt_{max}, and dp/dt_{min} were significantly increased whereas values of LVEDP remained not significantly different when control + AG-treated rats were compared with the control rats that received the vehicle (Table 1). On the contrary, values of LVSP, dp/dt_{max}, and dp/dt_{min} were significantly decreased whereas values of LVEDP were significantly increased in DOX-treated rats as compared to control rats, all of which were completely reversed in DOX + AG-treated rats. These data suggest a potent inotropic effect of AG in both control and DOX-treated rats (Table 1). Interestingly, values of all these hemodynamic parameters were not significantly different when DOX + AG + AG490, DOX + AG + [D-Lys3]-GHRP-6, and DOX + AG-treated rats were compared with each other (Table 1), suggesting that such an inotropic effect of AG involves stimulation of the AG receptors, GHSR1a, and JAK2 signaling pathway (Table 2).

Independent of food intake and changing body weight, but through GHSR1a and JAK2, AG prevents DOX-induced impairment in LV function and the increase in serum cardiac markers

There was no significant change in weekly food intake between all the experimental groups of the study among the 7 weeks period of the study (Fig. 1a, b). However, DOX-treated rats showed a significant decrease in their final body weights and weekly food intake, starting from weeks 4 and 2, respectively, and had significantly higher plasma levels of CK-MB and BNP 45, as compared to control rats (Fig. 1a–d). On the other hand, neither treatment of AG alone to control rats or to DOX-treated rats or administration of AG in combination with AG490 or with [D-Lys3]-GHRP-6 to DOX-treated rats affected the body weights and food intake of rats as compared to control or DOX-treated rats, respectively (Fig. 1a–d). While administration of AG did not affect plasma levels of CK-MB and BNP 45 in control rats, it significantly lowered them in the plasma of DOX + AG-treated rats, as compared to DOX-treated rats (Fig. 1c, d). However, similar non-significant plasma levels of CKMB and BNP 45 were seen when DOX, DOX + AG + AG490, and DOX + AG + [D-Lys3]-GHRP-6 were compared with each other, suggesting that the protective effect of AG on DOX-induced cardiotoxicicity is mediated by GHSR1a and requires activation of JAK2.

Table 2 Hemodynamic parameters in all experimental groups of part 2

	Control	Co + AG	DOX	DOX + AG	DOX + AG + AG490	DOX + AG + [D-Lys3]-GHRP-6
LVSP (mm Hg)	96.4 ± 7.2	121 ± 7.2[a]	67.2 ± 5.3[a,b]	89.5 ± 8.5[b,c]	63.4 ± 6.4[a,b,d]	68.5 ± 4.7[a,b,d]
LVEDP (mm Hg)	3.2 ± 0.7	3.1 ± 0.4	12.3 ± 1.3[a,b]	3.9 ± 0.7[b,c]	11.4 ± 0.9[a,b,d]	12.5 ± 1.0[a,b,d]
dp/dt_{max}	4122 ± 299	4964 ± 223[a]	1342 ± 109[a,b]	3911 ± 378[b,c]	1631 ± 311[a,b,d]	1234 ± 256[a,b,d]
dp/dt_{min}	3891 ± 231	4552 ± 353[a]	1119 ± 104[a,b]	3672 ± 311[b,c]	1381 ± 218[a,b,d]	1092 ± 178[a,b,d]
HR (beats/min)	334 ± 45.2	314 ± 34.7	365 ± 59.4	342 ± 38.4	331 ± 47.1	328 ± 32.3
AG (pg/ml)	122.7 ± 13.6	185 ± 22.1[a]	56.4 ± 11.6[a,b]	96.5 ± 9.9[b,c]	91.2 ± 8.6[a,b,c,d]	103 ± 10.4[a,b,c,d]

Data are presented as mean ± SD of $n = 8$ rats/group

AG, acylated ghrelin; DOX, doxorubicin; AG490, a JAK2 inhibitor; [D-Lys3]-GHRP-6, an AG receptor (GHSR1a) antagonist

[a] Significantly different as compared with the control group

[b] Significantly different as compared to the control + AG-treated group

[c] Significantly different as compared to the DOX-treated group

[d] Significantly different as compared to the DOX + AG-treated group

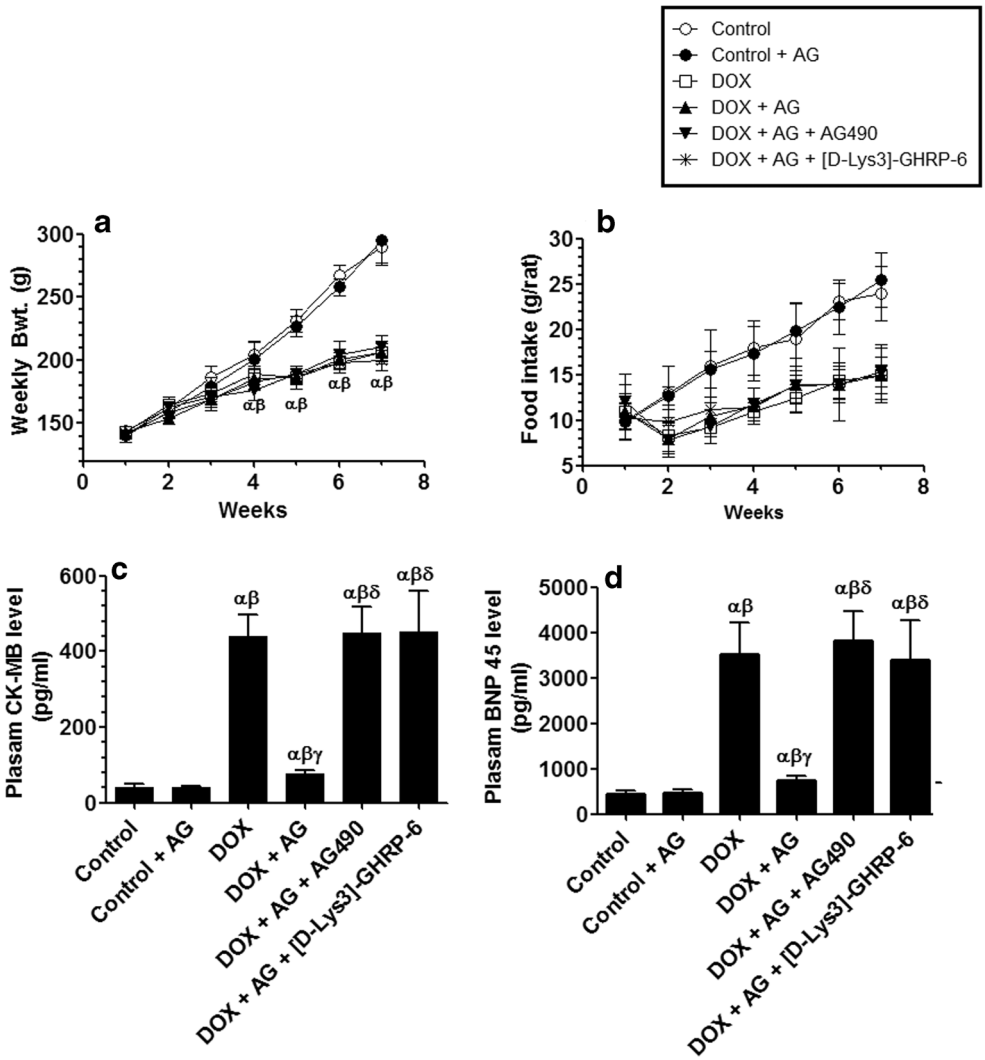

Fig. 1 Changes in final body weights (**a**), food intake (**b**), plasma CK-MB (**c**), and BNP-45 (**d**) in all groups of rats. Data are presented as mean ± SD of $n = 8$ rats/group. $^{\alpha}$, significantly different as compared with the control group; $^{\beta}$, significantly different as compared to the control + AG-treated group; $^{\delta}$, significantly different as compared to the DOX + AG-treated group; AG, acylated ghrelin; DOX, doxorubicin; AG490, a JAK2 inhibitor; [D-Lys3]-GHRP-6, an AG receptor (GHSR1a) antagonist

AG enhances GSH levels but has no effect on IL-6 expression in the LVs of both control and DOX-treated rats

Left ventricles (LVs) of DOX-treated rats showed significantly lower levels of GSH with parallel higher levels of ROS and mRNA and protein levels of IL-6, as compared to control rats (Fig. 2a–d). Control + AG or DOX + AG-treated rats showed significantly higher content of GSH in their LVs as compared to control or DOX-treated rats, respectively (Fig. 2a). However, levels of ROS and mRNA and protein levels of IL-6 remained statistically not significant between control and control + AG-treated rats (Fig. 2c–d). Administration of either AG490 or [D-Lys3]-GHRP-6 to DOX + AG-treated rats did not affect mRNA and protein levels of IL-6 but significantly lowered GSH levels and increased ROS in the LVs of rats as compared to DOX-treated rats (Fig. 2a, b). The levels of all these biochemical markers were not significantly different when DOX + AG + AG490, DOX + AG + [D-Lys3]-GHRP-6, and DOX-treated rats were compared with each other (Fig. 2a–d). These data suggest that the AG exerts an antioxidant potential in the heart of rats, at least, by enhancing endogenous GSH levels, an effect that requires activation of GHSR1a and of JAK2.

AG inhibits mRNA and protein levels of collagen 1/III and TGF-β1 in the LVs of DOX-treated rats

mRNA and protein levels of collagen I, collagen III, and TGF-β1 were not statistically different in LVs of control and control + AG-treated rats (Fig. 3a–d). However, mRNA and protein levels of collagen 1, collagen III, and TGF-β1 were significantly increased in LVs of DOX-treated rats as compared to control rats (Fig. 3a–d). On the other hand, mRNA and protein levels of collagen 1, collagen III, and TGF-β1 were significantly decreased in the LVs of DOX + AG as compared to DOX-treated rats, effects that were completely abolished when DOX + AG-treated rats were co-administered either G490 and DOX + [D-

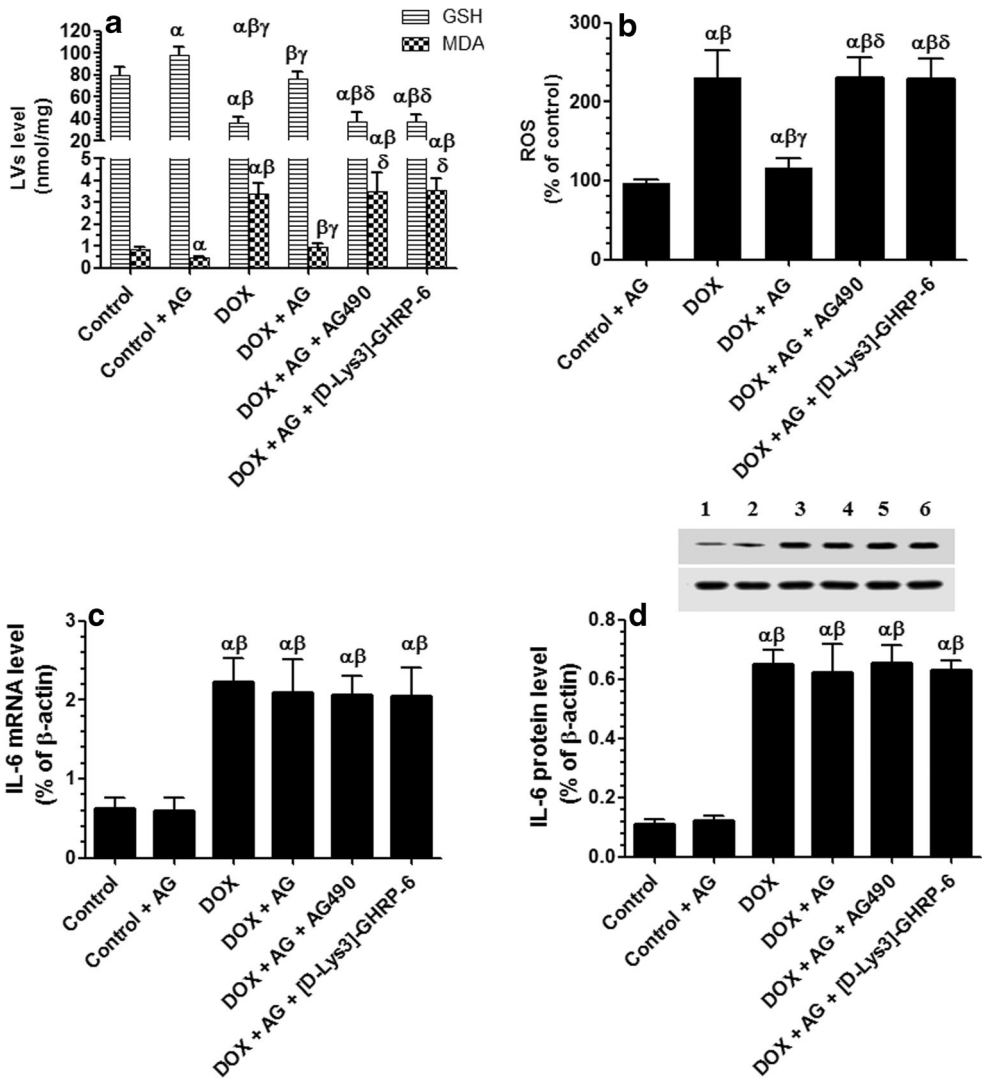

Fig. 2 Levels of reduced glutathione (**a**) and malondialdehyde (MDA, **a**), reactive oxygen species (ROS, **b**), mRNA of IL-6 (**c**), and protein levels of IL-6 (**d**) in left ventricles (LVs) of all groups of rats. Data are presented as mean ± SD of $n = 6$ rats/group. $^{\alpha}$, significantly different as compared with the control group; $^{\beta}$, significantly different as compared to the control + AG-treated group; $^{\delta}$, significantly different as compared to the DOX + AG-treated group; AG, acylated ghrelin; DOX, doxorubicin; AG490, a JAK2 inhibitor; [D-Lys3]-GHRP-6, an AG receptor (GHSR1a) antagonist

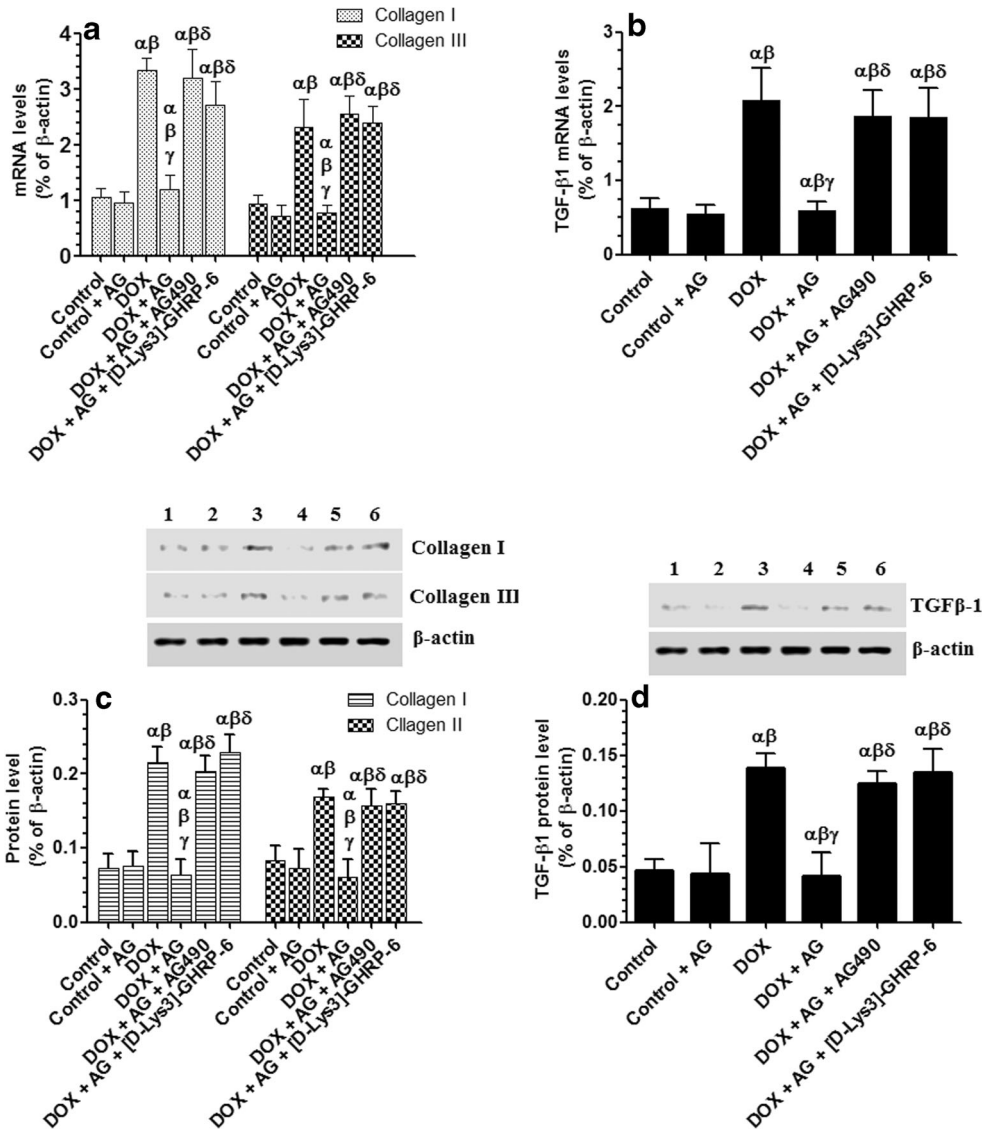

Fig. 3 mRNA and protein levels of collagen 1 and III (**a**, **c**) and transforming growth factor-β1 (TGF-β1, **b**, **d**) in left ventricles (LVs) of all groups of rats. Data are presented as mean ± SD of $n = 6$ rats/group. $^{\alpha}$, significantly different as compared with the control group; $^{\beta}$, significantly different as compared to the control + AG-treated group; $^{\delta}$, significantly different as compared to the DOX + AG-treated group; AG, acylated ghrelin; DOX, doxorubicin; AG490, a JAK2 inhibitor; [D-Lys3]-GHRP-6, an AG receptor (GHSR1a) antagonist

Lys3]-GHRP-6 (Fig. 3a–d). These data suggest that the inhibitory effect of AG on the expression of collagen 1, collagen III, and TGF-β1 in the LVs of DOX-treated rats is GHSR1a- and JAK2-dependent. However, there were no significant changes in mRNA and protein levels of collagen I, collagen III, and TGF-β1 between DOX, DOX + AG + AG490, and DOX + AG + [D-Lys3]-GHRP-6 when compared to each other or with DOX-treated rats (Fig. 3a–d).

AG inhibits collagen deposition in DOX-treated LVs

Cardiac myocytes of LV sections from both control and control + AG showed few collagen fibers between the cardiac muscle fibers and around blood vessels (Fig. 4a, b). Sections from the DOX-treated group revealed an obvious increase in collagen fiber deposition which appeared very dense, wavy, spiral, and thick bundles in between the cardiac muscle fibers and around blood vessels (Fig. 4c). In addition, focal areas of collagen fibers replaced some degenerated parts of the cardiac muscle fibers. Sections from DOX + AG-treated rats showed a reduction in collagen fibers as compared to DOX-treated rats. Like the control, these few collagen fibers appeared between the regularly arranged cardiac muscle (Fig. 4d). However, LVs of DOX + AG + AG490 and DOX + AG + [D-Lys3]-GHRP-6-treated rats (Fig. 4e, f) showed an increase in collagen fiber deposition that looks similar in quantity, shape, and distribution to that observed in DOX-treated rats (Fig. 4f).

AG enhances JAK2 and ERK1/2 activity and inhibits P38 activity in the LVs of both control and DOX-treated rats

There were no significant changes in the LV total protein levels of JAK1, JAK2, and ERK1/2 as well as in protein levels

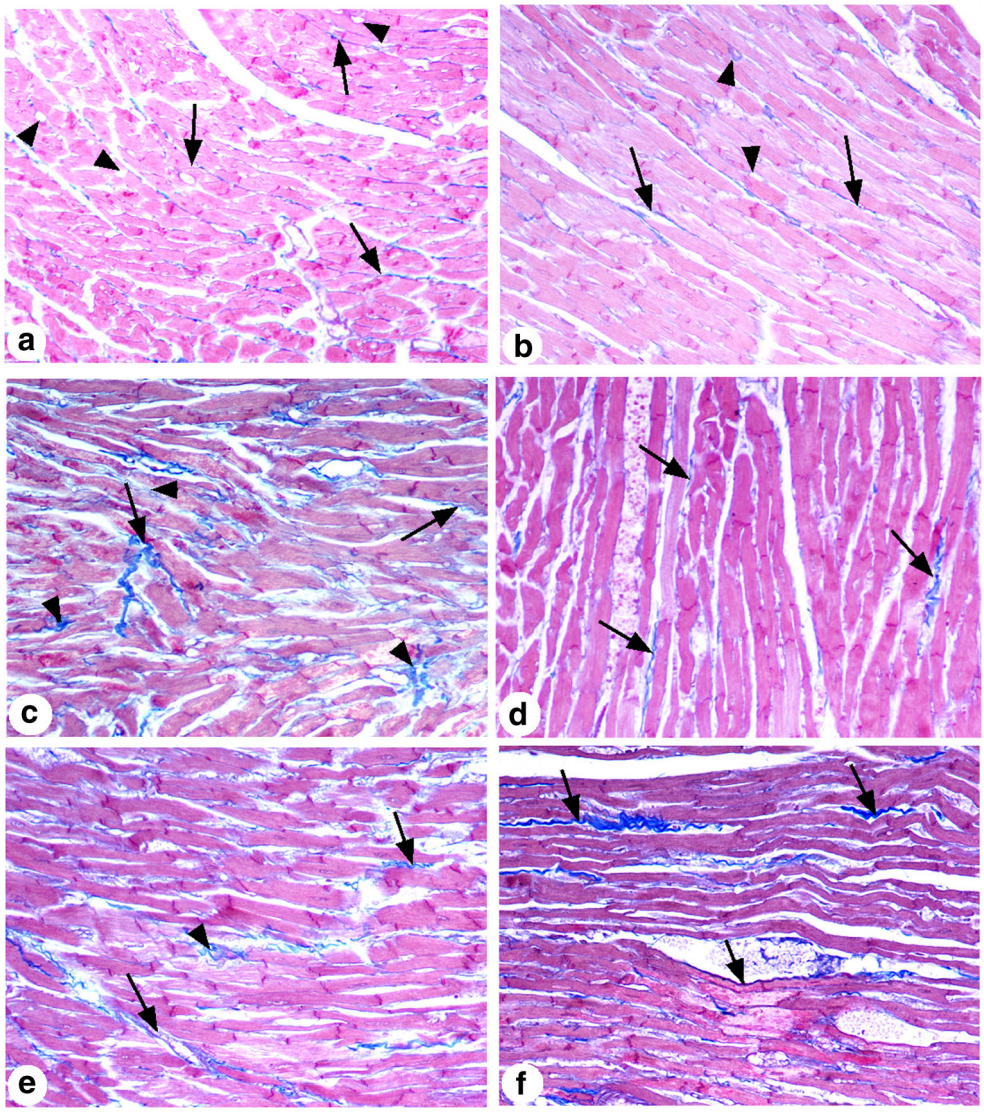

Fig. 4 Photomicrographs of Masson's trichrome stainings of left ventricles of all groups of rats. **a**, **b** Taken from control and control + AG-treated rats, respectively, which both show few collagen fibers accumulated between the cardiac muscle fibers (arrows) and around blood vessels (arrow heads). **c** Taken from a DOX-treated rat and shows an obvious increase in collagen fibers which looks very dense, wavy, spiral, and thick bundles located between the cardiac muscle fibers (arrows). In some places, degenerated parts of the cardiac muscle fibers were replaced by collagen fibers (arrow heads). **d** Taken from a DOX + AG-treated rat and shows a very clear reduction in collagen fibers accumulation which is located between the cardiac muscles fibers (arrows). **e**, **f** Taken from DOX + AG + AG490 and DOX + AG + [D-Lys3]-GHRP-6-treated rats and show an obvious increase in collagen fibers deposition between the cardiomyocytes (arrows) or replacing the degenerated areas of the cardiac muscle fibers (arrow heads). 200×

of p-JAK1 p-JAK1 ($Tyr^{1034/1035}$) between all groups of rats (Fig. 5a–d). Left ventricular (LV) protein levels of p-JAK 2 ($Tyr^{1007/1008}$) and p-ERK1/2 were significantly reduced, but protein levels of P38 were significantly increased in DOX-treated rats as compared to control rats (Fig. 5a, c, d). However, administration of AG to control or DOX-treated rats significantly increased protein levels of p-JAK2 ($Tyr^{1007/1008}$) and p-ERK1/2 and significantly lowered protein levels of P38 (Fig. 5a, c, d). Interestingly, protein levels of p-JAK 2 ($Tyr^{1007/1008}$) and p-ERK1/2 and protein levels of P38 were not significantly different between DOX, DOX + AG490, and DOX + [D-Lys3]-GHRP-6-treated rats (Fig. 5a, c, d). These data suggest that AG stimulates ERK signaling and inhibits that of P38 through activation of JAK2 and requires GHSR1a.

AG enhances levels and activity of STAT3 and inhibits levels and activity of STAT1 in the LVs of both control and DOX-treated rats

Total protein levels of STAT3 and p-STAT3 (Tyr^{705} & Ser^{727}) were significantly decreased whereas total protein levels of STAT1 and p-STAT1 (Tyr^{701} & Ser^{727}) were significantly increased in LVs of DOX-treated rats as compared to control (Fig. 6a–d). However, administration of AG to either control

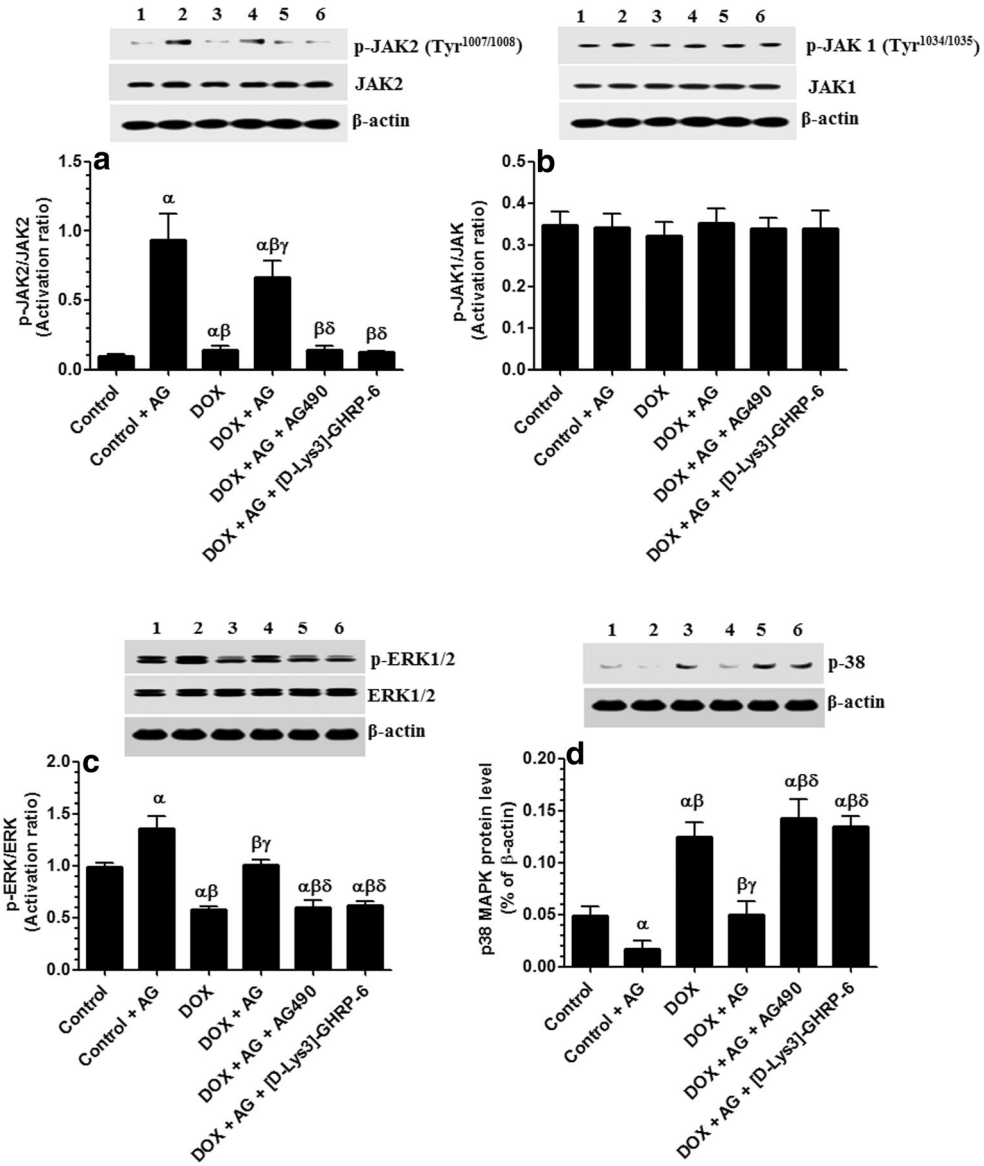

Fig. 5 Protein levels of total and phospho-JAK1 (Tyr$^{1034/1035}$) (**a**), total and phosphor-JAK2 (Tyr 1007/1008) (**b**), total and phosphor-ERK1/2 (**c**), and P38 (**d**) in left ventricles (LVs) of all groups of rats. Data are presented as mean ± SD of $n = 6$ rats/group. $^{\alpha}$, significantly different as compared with the control group; $^{\beta}$, significantly different as compared to the control + AG-treated group; $^{\delta}$, significantly different as compared to the DOX + AG-treated group; AG, acylated ghrelin; DOX, doxorubicin; AG490, a JAK2 inhibitor; [D-Lys3]-GHRP-6, an AG receptor (GHSR1a) antagonist

or DOX-treated rats significantly increased total STAT3 and p-STAT3 (Tyr^{705} & Ser^{727}) and significantly increased protein levels of STAT1 and p-STAT1 (Tyr^{701} & Ser^{727}) (Fig. 6a–d). A similar picture of changes in the protein levels of total and phosphorylated forms of both STAT1 and STAT 3 seen in DOX-treated rats was also seen in both DOX + AG490 and DOX + [D-Lys3]-GHRP-6-treated rats (Fig. 6a–d), suggesting that the stimulatory effect of AG on levels and activities of STAT1/3 is mediated through GHSR1a and activation of JAK2.

AG upregulates the protein levels of Bcl-2 and downregulates those of Bax and cleaved caspase-3 in the LV of control and DOX-treated rats

Protein levels of Bax and cleaved caspase-3 were significantly increased, while protein levels of Bcl2 were significantly reduced in LVs of DOX-treated rats (Fig. 7a–c). Similarly, immunoreactivity of cleaved caspase-3 was also increased in the cytoplasm of the cardiomyocytes of the LVs of DOX-treated rats (Fig. 8c). Protein levels of Bcl2 were significantly increased, and protein levels of Bax and cleaved caspase-3 were significantly reduced in LVs of both control + AG and DOX + AG-treated rats as compared to control or DOX-treated rats, respectively (Fig. 7a–c). Also, cleaved caspase-3 immunoreactivity was reduced in DOX + AG-treated rats as compared to control rats (Fig. 8d). Of note, co-administration of AG490 or DOX + [D-Lys3]-GHRP-6 to DOX + AG-treated rats completely abolished the stimulatory effect of AG on Bcl-2 protein levels and its inhibitory effect on Bax and cleaved caspase-3 protein levels or cleaved caspase-3 immunoreactivity, and their levels were not statistically different to those observed in DOX-treated rats (Figs. 6a–c and 8e, f).

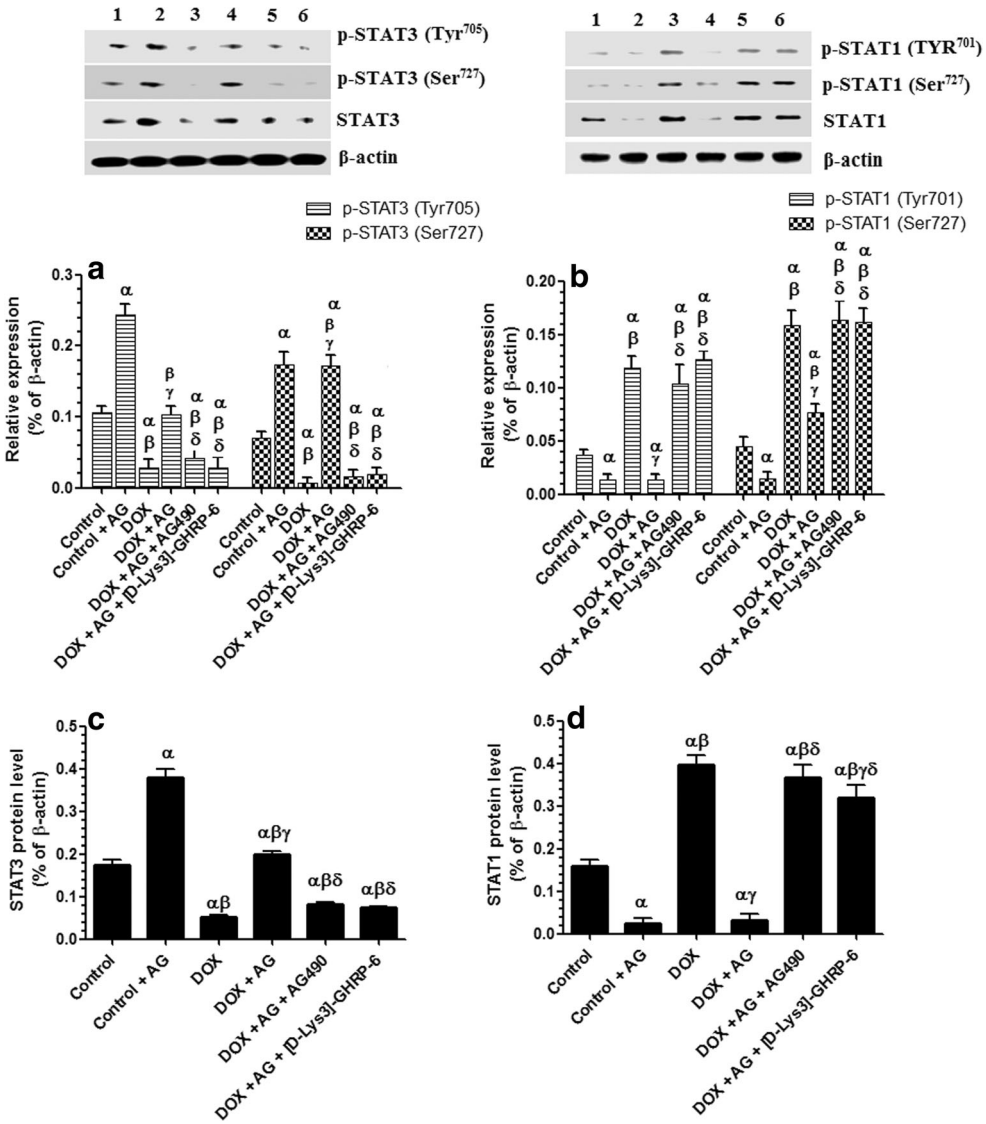

Fig. 6 Protein levels of total and phospho-STAT1 (Tyr^{701,} Ser^{727,}) (**a**, **c**) and total and phosphor-STAT3 (Tyr^{705,} Ser^{727}) (**b**, **d**) in left ventricles (LVs) of all groups of rats. Data are presented as mean ± SD of $n = 6$ rats/group. $^{\alpha}$, significantly different as compared with the control group; $^{\beta}$, significantly different as compared to the control + AG-treated group; $^{\delta}$, significantly different as compared to the DOX + AG-treated group; AG, acylated ghrelin; DOX, doxorubicin; AG490, a JAK2 inhibitor; [D-Lys3]-GHRP-6, an AG receptor (GHSR1a) antagonist

AG improves cardiomyocytes and mitochondrial features and inhibits cell apoptosis and collagen deposition as depicted by ultrastructure images

Left ventricle (LVs) of control and control + AG-treated rats showed well-preserved normal myocyte structure, abundant healthy striated myofibrils, and intact mitochondria with very few collagens in the intercellular spaces between plasma membranes (Fig. 8a, b). On the other hand, rats administered DOX showed severe degeneration in their myocytes, myofibrils, and mitochondria with loss of the normal striation and increased accumulation of collagen fibers. Apoptotic bodies in cardiac cells were also clearly observed (Fig. 8c). On the other hand, almost normal ultrastructures with preserved cardiac myocytes, mitochondrial, and myofibrils and reduced collagen deposition were seen in LV of DOX + AG-treated rats (Fig. 8d). However, similar pictures to that of DOX-treated rats were seen in the left ventricles of DOX + AG + AG490 or DOX + AG + [D-Lys3]-GHR-6-treated rats (Figs. 8e, f and 9).

Discussion

The evidence presented in this study is the first to show that DOX-induced apoptosis and fibrosis in the LVs of rats is associated with decreased and increased activity and expression STAT3 and STAT1, respectively. Concomitantly, it increased protein levels of IL-6 and p38 MAPK and decreased the activities of p-ERK1/2, major STAT1, and STAT3 serine kinases, respectively. Hence, DOX shifted normal cardiac signaling of IL-6/JAK2/STAT3 toward IL-6/JAK2/STAT1 signaling. It also demonstrates that co-administration of AG is able to protect the cardiomyocytes from DOX-induced apoptosis and fibrosis by activation of

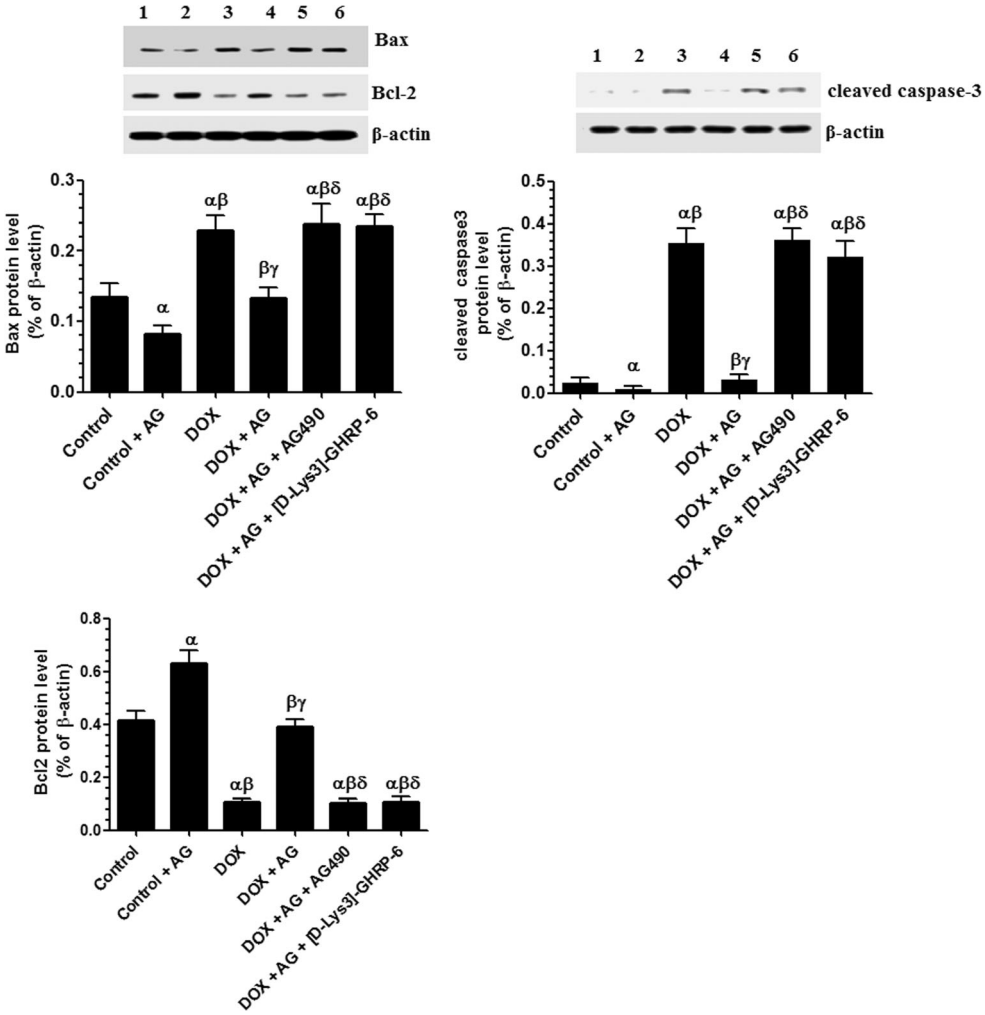

Fig. 7 Protein levels of Bax (**a**), cleaved caspase-3 (**b**), and Bcl2 (**c**) in left ventricles (LVs) of all groups of rats. Data are presented as mean ± SD of $n = 6$ rats/group. $^{\alpha}$, significantly different as compared with the control group; $^{\beta}$, significantly different as compared to the control + AG-treated group; $^{\delta}$, significantly different as compared to the DOX + AG-treated group; AG, acylated ghrelin; DOX, doxorubicin; AG490, a JAK2 inhibitor; [D-Lys3]-GHRP-6, an AG receptor (GHSR1a) antagonist

JAK2, stimulation of STAT3 expression and activity, and inhibition of STAT1, an effect that is mediated through GHSR1a and independent of IL-6.

The first confirmatory observation for the validity of cardiotoxicity in the DOX-rat model of this study was evident by the significant reduction in rats' final body weight and food intake, which both are in accordance with other previous clinical and experimental studies (Desai et al. 2013; Deepak et al. 2016; Kihara et al. 2016). Ghrelin O-acyl transferase enzyme (GOAT) is the major enzyme responsible for ghrelin acylation (Al Massadi et al. 2011). Interestingly, we have also found a significant decrease in the level of AG in the plasma of DOX-treated rats, suggesting that DOX either can destroy the ghrelin-secretory cells in the stomach or inhibit acylation of AG by inhibition of GOAT. Normally, AG stimulates food intake and adiposity (Kojima et al. 2001). Hence, the decrease in circulatory AG levels in DOX-treated rats may explain the significant reduction in the weights and food intake in these rats. However, exogenous administration of AG was shown to prevent DOX-induced decrease in food intake and weight loss in cancer patients and animals (Hiura et al. 2012; Wang et al. 2014; Kihara et al. 2016), an effect that was not seen in this study. This is basically could be attributed to the dose of AG used, treatment period, and severity of the condition. Similar to these findings, other authors who used a similar dose of AG in other animal models have shown no effect on weights of rats (Işeri et al. 2008; Li et al. 2013). However, these data suggest that all other physiological and biochemical alterations observed in all groups treated with AG are independent of food intake or weight loss.

On the other hand, it was shown that DOX-induced ROS and intrinsic apoptosis and fibrosis contribute significantly to its cardiovascular damaging effect (Kumar et al. 2001; Wallace 2003; Octavia et al. 2012; Accornero et al. 2015; Pei et al. 2015). In the same line, the cardiotoxic effect of DOX on the LVs of treated rats was confirmed by the impaired systolic and diastolic function, elevated circulatory levels of cardiac markers (CKMB and BNP-45), the severe damage in their microtubules and mitochondria, upregulation of TGF-β1, and increased synthesis and deposition of collagen. Also, mitochondria-mediated apoptosis was evident in the LVs of these rats by the damaged mitochondria, the

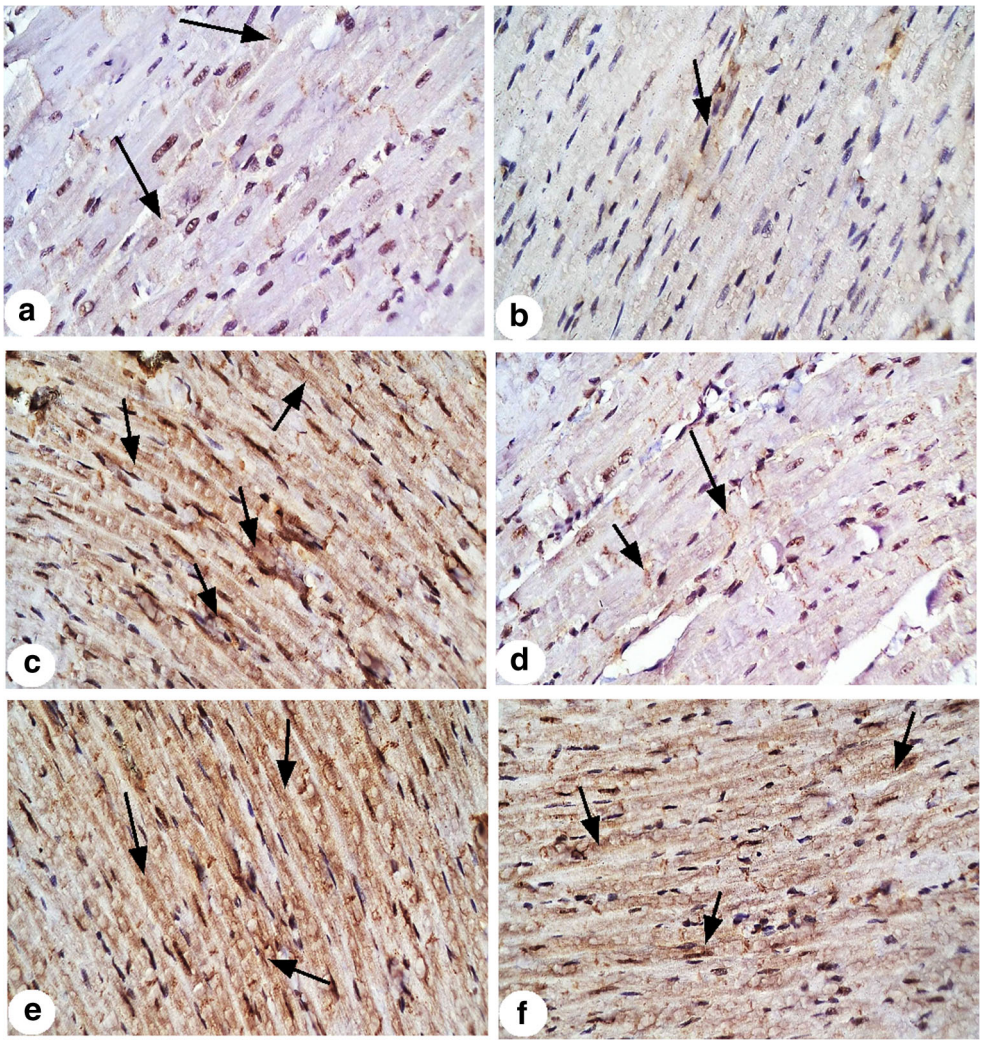

Fig. 8 Expression of active caspase-3 in the left ventricles (LVs) of all groups of rats as detected by immunohistochemistry. **a**, **b** Taken from control and control + AG-treated rats, respectively, and show weak immunoreactivity of active caspase-3 in the cytoplasm of the cardiomyocytes (arrows). **c** Taken from a DOX-treated rat and shown very strong cytoplasmic immunoreactivity of active caspase-3 in the cytoplasm of the cardiomyocytes (arrows). **d** Taken from a DOX + AG-treated rats and shows a weak cytoplasmic immunoreactivity of active caspase-3. **e**,**f** Taken from DOX + AG + AG490 and DOX + AG + [D-Lys3]-GHRP-6-treated rats and shows a similar picture to that observed in the DOX-treated rats

upregulation and increased immunoreactivity of cleaved caspase-3 (and immunoreactivity), the upregulation of Bax, and the lowered protein levels of Bcl-2. These changes can be attributed to DOX-induced overproduction of ROS and depletion of GSH levels as shown in the LVs of these rats.

Indeed, it was shown that ROS generated by DOX induces intrinsic cell death in the cardiomyocytes by several mechanisms including activation of p53 tumor suppressor, c-Jun N-terminal kinase (JNK), and p38 MAPK, which all lead to increasing Bax expression and translocation to the mitochondrial and by downregulation of the transcriptional factor, GATA-4, leading to decreased Bcl-XL and Bcl-2 expression (Aries et al. 2004; L'Ecuyer et al. 2006; Shizukuda et al. 2005; Poizat et al. 2005; Lou et al. 2005). In the same line, in this study and associated with the above-mentioned alteration in the apoptotic markers, DOX damaged the myocardium mitochondria, increased the activity of P38 MAPK, and inhibited that of ERK1/2 (Lee et al. 2002; Li et al. 2003; Lu and Xu 2006). Interestingly, p38 MAPK and ERK1/2 can inversely affect the activity of each other within the cells (Berra et al. 1998; Li et al. 2003). Hence, we are still unsure whether DOX-induced inhibition of ERK1/2 triggered the activation of p38 or vice versa.

On the other hand, the antioxidant, anti-apoptotic, and anti-fibrotic effects of AG were also confirmed in the LVs of DOX-treated rats, where co-administration of AG prevented the DOX-induced cardiac cell damage and inhibited cardiac fibrosis and intrinsic apoptosis associated with reducing ROS generation, boosting GSH levels, activation of ERK1/2, and inhibition of P38MAPK. These findings are in the same line to those previously described by Baldanzi et al. (2002) and Pei et al. (2014). Interestingly, the stimulatory effect of AG on GSH and ERK1/2 and its inhibitory effect on P38 MAPK were shown in the LVs of both control and DOX-treated rats. This could explain why the LVs of both groups of rats have lower protein levels of Bax and cleaved caspase-3 and higher levels of Bcl-2.

In addition, supporting to our findings, AG augments the endogenous antioxidant system in hearts of rats and activated ERK1/2 in other cell types via several mechanisms including

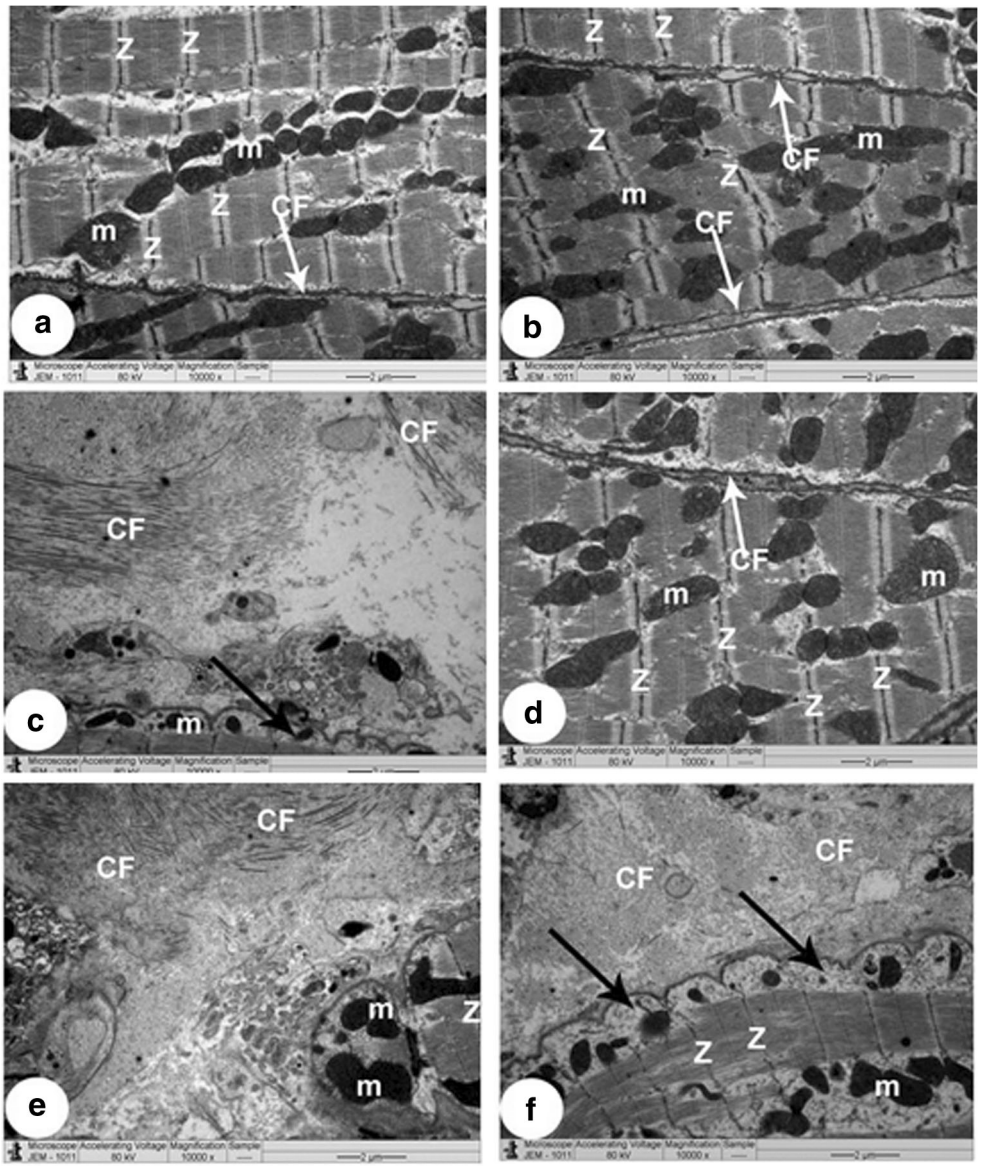

Fig. 9 Transmission electron micrographs obtained from all group of rats. **a**, **b**, **d** Taken from the control, control + AG, or DOX + AG-treated rats, respectively, and showing rats normal myocyte structure with dense cytoplasm filled with healthy striated myofibrils with clear bands (Z and H). The mitochondria look intact mitochondria (m) with generally distinct cristae and normal matrix. Very few collagen fibers (CF) were seen in the intercellular spaces between plasma membranes. **c**,**e**,**f** Taken from DOX, DOX + AG + AG490, or DOX + AG + [D-Lys3]-GHRP-6, respectively, and showing pleomorphic myocyte structure with degenerated myofibrils and damaged in bands (Z and H) as well as damaged mitochondria (m). Black arrows pointed to blebs in the apoptotic cardiac cells. Expansion of the interstitial space between plasma membranes and dense accumulation of collagen fibrils (CF) were also well seen. 200×

activation of JAK2 (Nanzer et al. 2004), PKC (Mousseaux et al. 2009), and cyclic adenosine monophosphate (cAMP)/protein kinase A (PKA) pathway (Granata et al. 2007; Rossi et al. 2009; Pipicz et al. 2018). Given the increase in the activity of JAK2 in the heart of control or DOX-treated animals which were co-treated with AG (as discussed later), it is most likely that AG enhanced GSH and ERK1/2 activity in the LVs of treated rats through activation of the JAK2 pathway. Indeed, inhibition of JAK2 in the DOX + AG-treated rats of this study completely abolished the stimulatory effects of AG on GSH and ERK1/2 activity. This may highlight the importance of the JAK2/ERK1/2 axis in the anti-apoptotic and antioxidant role of AG in the heart. However, given that no alterations in JAK 2 activity were observed in DOX-treated rats, it is reasonable that such decrease in cardiac levels of GSH is a result of overconsumption due to DOX-induced overproduction of ROS.

These data encouraged us to go further and investigate the expression pattern and role of major JAK/STAT family members in the process of DOX-induced cardiac toxicity and the protective effect of AG. The interesting finding of this study is that we have found significant decrease in the total protein levels of STAT3 and p-STAT3 (Tyr^{705} and Ser^{727}) with parallel increases in total STAT1 and p-STAT-1 (Tyr^{701} and Ser^{727}), as well as an increase in mRNA and protein levels of IL-6 in the LVs of DOX-treated rats. As mentioned previously, there were no alterations in levels of p-JAK2 ($Tyr^{1007/1008}$) nor p-JAK1 ($Tyr^{10034/1035}$). These data suggest that the fibrotic and apoptotic effects of DOX could be mediated through activation of IL-6/STAT1 axis and inhibition of STAT3.

The increase in cardiac IL-6 has been also described previously in the hearts of DOX-treated rats (Sauter et al. 2011; Hong et al. 2017). On the other hand, although the regulation of STAT is usually regulated by phosphorylation, the decrease in total STAT3 and the increase in total STAT1, in the heart of DOX-treated rats can be supported by other previous observations. Indeed, mRNA of STAT3 was significantly decreased in the hearts of mice after DOX treatment (Kunisada et al. 2000). In addition, decreased levels of total STAT-3 and p-STAT-3 with a reduced number of STAT-3-positive cardiomyocytes were seen in the heart of patients with failing heart (Podewski et al. 2003). At this stage, we are still unable to explain the precise mechanisms responsible for the alteration in total protein levels of these STAT members, and further investigation is needed.

However, regardless of the role of JAK1/2 in STAT3 phosphorylation, phosphorylation of serine residues of STAT1 and STAT3 can be also induced by P38 and ERK1/2, respectively (Barry et al. 2007). Hence, it will be logic to explain the significant increase in p-STAT1 and the decrease in p-STAT3 (both at Ser^{727}) in the LVs of DOX-treated rats by the parallel increase in P38 levels and the significant decrease in the activity of ERK1/2, respectively. Additionally, the decrease in p-STAT-3 (Tyr^{705}) in LVs of DOX-treated rats can be also explained by the observed decrease in total levels of STAT3 post-DOX therapy. However, it looks unnormal to observe a decrease in p-STAT3 with the presence of high levels of IL-6, which is a potent inducer of STAT3. In fact, STAT-1 and STAT-3 can negatively affect the expression of each other (Stephanou et al. 2000; Barry et al. 2007), suggesting DOX-induced increased expression in STAT1 inhibited the expression and activity of STAT3 and vice versa. Intriguingly, although STAT1 and STAT3 are activated by different ligands, in the absence or in the decrease of STAT-3 levels, IL-6 signaling can be switched to an IFN-γ-like effect which results in sustained activation of STAT-1 (Costa-Pereira et al. 2002), resembling a perfect match of the picture between our hands.

On the other hand and with no alteration in cardiac mRNA and protein levels of IL-6 but with significant increase in protein levels of p-JAK2 ($Tyr^{1007/1008}$), heart of control or DOX-treated rats which were co-administered with AG showed significant increase in STAT3 levels and activity of ERK1/2 with a concomitant significant decrease in level and activity of STAT-1 and activity of P38 MAPK, confirming the important regulatory effect of MAPK signaling in regulation of STAT1/3 activation and signaling. These data suggest that AG stimulates the synthesis and phosphorylation of STAT3 which may inversely inhibit the expression and activity of STAT1. However, such effect of AG seems to be JAK2.dependent. This has been confirmed in this study as the stimulatory effect of AG on STAT3 and its inhibition on STAT1 activity and levels were completely abolished by the administration of AG490. These findings suggest that the AG-cardioprotective effect is associated with increased signaling through IL-6/gp130/JAK2/STAT3. Similar to these findings, it was shown that AG, through JAK2, can protect against MI-induced HF by activation of STAT3 and inhibition of STAT1 activity (Eid et al. 2018).

However, how does AG increase JAK-2 phosphorylation in the control rats treated with AG in the absence of any stimulation of IL-6 remains a challenging question? In fact, this could be related to the alterations in MAPKs observed in this study. In addition, it is well-known that other IL-6-related cytokines (inhibitory factor, oncostatin M, ciliary neurotrophic factor, and cardiotrophin) (Fischer and Hilfiker-Kleiner 2008; Pipicz et al. 2018), growth factors, granulocyte colony-stimulating factor (G-CSF) (Harada et al. 2005), and other humoral factors, such as angiotensin II (ANG II) (Booz et al. 2002), can directly induce the activation of JAK2. Hence, it could be possible that AG acts by activating on more of these mediators. Also, another possibility could be explained by the effect AG on SOCS1/3 protein expression which is natural negative regulator of STAT1/3 in the cardiomyocytes. These suggestions could be a new area of future research and need further investigation.

In conclusion, the findings of this study are unique to show that DOX, through inducing oxidative stress, is able to induce cardiac intrinsic apoptosis and fibrosis by enhancing apoptosis and fibrosis through activation of IL-6/STAT1 axis and inhibition of STAT3 signaling. However, AG is a protective agent against DOX-induced toxicity mainly due to its ability to increase GSH levels and inhibit fibrosis and the intrinsic cell death by activation of STAT3 and inhibition of STAT1, effects that are mediated through its own receptors, GHSR1a, and require activation of JAK2.

Acknowledgments The authors would like to thank the animal facility staff at the King Khalid University (KKU), Abha, KSA, for their help in taking care of the animals, treatment, and blood tissue collection. They would like also to thank Mr. Mahmoud Alkhateeb from the College of Medicine at King Saud University of Health Sciences and the technical staff members of the Physiology and Biochemistry in the College of Medicine at KKU for their contribution in the recording of the cardiovascular function of the experimental groups and helping in the determination of some biochemical parameters. Furthermore, the authors would like to thank Dr. Reffat Eid, from the Pathology Department at the College of Medicine in KKU for his significant contribution in the histology, immunohistochemistry, and electron microscopy studies. The authors extend their appreciation to the Deanship of Scientific Research at King Khalid University for funding this work through the research group program under grant number (R.G.P.1 /40/39).

Author contributions AS conceived and designed the research. AS and AFE conducted the experiments. AS analyzed and graphed the data. AS and AFEK wrote and revised the manuscript. AS and AFE read and approved the final version of the manuscript.

Funding This study was funded by the Deanship of Scientific Research at King Khalid University, Abha, Saudi Arabia (grant number R.G.P.1/40/39).

Compliance with ethical standards

All applicable international, national, and/or institutional guidelines for the care and use of animals were followed. All procedures performed in studies involving animals were in accordance with the ethical standards for the use and care of laboratory animals at King Khalid University, Abha, KSA.

Conflict of interest The authors declare that they have no conflict of interest.

References

Accornero F, van Berlo JH, Correll RN, Elrod JW, Sargent MA, York A, Rabinowitz JE, Leask A, Molkentin JD (2015) Genetic analysis of connective tissue growth factor as an effector of transforming growth factor β signaling and cardiac remodeling. Mol Cell Biol 35:2154–2164

Al Massadi O, Tschöp MH, Tong J (2011) Ghrelin acylation and metabolic control. Peptides 32:2301–2308

Aries A, Paradis P, Lefebvre C, Schwartz RJ, Nemer M (2004) Essential role of GATA-4 in cell survival and drug-induced cardiotoxicity. Proc Natl Acad Sci U S A 101:6975–6980

Baldanzi G, Filigheddu N, Cutrupi S, Catapano F, Bonissoni S, Fubini A, Malan D, Baj G, Granata R, Broglio F (2002) Ghrelin and des-acyl ghrelin inhibit cell death in cardiomyocytes and endothelial cells through ERK1/2 and PI 3-kinase/AKT. J Cell Biol 159:1029–1037

Barry SP, Townsend PA, Latchman DS, Stephanou A (2007) Role of the JAK–STAT pathway in myocardial injury. Trends Mol Med 13:82–89

Berra E, Diaz-Meco MT, Moscat J (1998) The activation of p38 and apoptosis by the inhibition of Erk is antagonized by the phosphoinositide 3-kinase/Akt pathway. J Biol Chem 273:10792–10797

Bisi G, Podio V, Valetto MR, Broglio F, Bertuccio G, Aimaretti G, Pelosi E, Del Rio G, Muccioli G, Ong H, Boghen MF, Deghenghi R, Ghigo E (1999) Cardiac effects of hexarelin in hypopituitary adults. Eur J Pharmacol 381:31–38

Booz GW, Day JN, Baker KM (2002) Interplay between the cardiac renin angiotensin system and JAK-STAT signaling: role in cardiac hypertrophy, ischemia/reperfusion dysfunction, and heart failure. J Mol Cell Cardiol 34:1443–1453

Bressenot A, Marchal S, Bezdetnaya L, Garrier J, Guillemin F, Plénat F (2009) Assessment of apoptosis by immunohistochemistry to active caspase-3, active caspase-7, or cleaved PARP in monolayer cells and spheroid and subcutaneous xenografts of human carcinoma. J Histochem Cytochem 57:289–300

Chang L, Ren Y, Liu X, Li WG, Yang J, Geng B, Weintraub NL, Tang C (2004a) Protective effects of ghrelin on ischemia/reperfusion injury in the isolated rat heart. J Cardiovasc Pharmacol 43:165–170

Chang L, Zhao J, Li GZ, Geng B, Pan CS, Qi YF, Tang CS (2004b) Ghrelin protects myocardium from isoproterenol-induced injury in rats. Acta Pharmacol Sin 25:1131–1137

Costa-Pereira AP, Tininini S, Strobl B, Alonzi T, Schlaak JF, Is' harc H, Gesualdo I, Newman SJ, Kerr IM, Poli V (2002) Mutational switch of an IL-6 response to an interferon-γ-like response. Proc Natl Acad Sci U S A 99:8043–8047

Dai B, Cui M, Zhu M, Su W-L, Qiu M-C, Zhang H (2013) STAT1/3 and ERK1/2 synergistically regulate cardiac fibrosis induced by high glucose. Cell Physiol Biochem 32:960–971

Deepak C, Saroj K, Surendra Kumar S, Man Kumar T, Soumya B, Chandra Bhushan J (2016) Effect of doxorubicin on histomorphology of liver of Wistar albino rats. JPP 4:186–190

Desai VG, Herman EH, Moland CL, Branham WS, Lewis SM, Davis KJ, George NI, Lee T, Kerr S, Fuscoe JC (2013) Development of doxorubicin-induced chronic cardiotoxicity in the B6C3F1 mouse model. Toxicol Appl Pharmacol 266:109–121

Eid RA, Alkhateeb MA, Eleawa S, Al-Hashem FH, Al-Shraim M, El-Kott AF, Zaki MSA, Dallak MA, Aldera H (2018) Cardioprotective effect of ghrelin against myocardial infarction-induced left ventricular injury via inhibition of SOCS3 and activation of JAK2/STAT3 signaling. Basic Res Cardiol 113:13

Fischer P, Hilfiker-Kleiner D (2008) Role of gp130-mediated signalling pathways in the heart and its impact on potential therapeutic aspects. Br J Pharmacol 153:S414–S427

Frascarelli S, Ghelardoni S, Ronca-Testoni S, Zucchi R (2003) Effect of ghrelin and synthetic growth hormone secretagogues in normal and ischemic rat heart. Basic Res Cardiol 98:401–405

Granata R, Settanni F, Biancone L, Trovato L, Nano R, Bertuzzi F, Destefanis S, Annunziata M, Martinetti M, Catapano F (2007) Acylated and unacylated ghrelin promote proliferation and inhibit apoptosis of pancreatic beta-cells and human islets: involvement of 3′,5′-cyclic adenosine monophosphate/protein kinase a, extracellular signal-regulated kinase 1/2, and phosphatidyl inositol 3-kinase/Akt signaling. Endocrinology 148:512–529

Harada M, Qin Y, Takano H, Minamino T, Zou Y, Toko H, Ohtsuka M, Matsuura K, Sano M, Nishi J-i (2005) G-CSF prevents cardiac remodeling after myocardial infarction by activating the Jak-Stat pathway in cardiomyocytes. Nat Med 11:305–311

Hilfiker-Kleiner D, Hilfiker A, Fuchs M, Kaminski K, Schaefer A, Schieffer B, Hillmer A, Schmiedl A, Ding Z, Podewski E (2004) Signal transducer and activator of transcription 3 is required for myocardial capillary growth, control of interstitial matrix deposition, and heart protection from ischemic injury. Circ Res 95:187–195

Hiura Y, Takiguchi S, Yamamoto K, Takahashi T, Kurokawa Y, Yamasaki M, Nakajima K, Miyata H, Fujiwara Y, Mori M, Kangawa K, Doki Y (2012) Effects of ghrelin administration during chemotherapy with advanced esophageal cancer patients: a prospective, randomized, placebo-controlled phase 2 study. Cancer 118:4785–4794

Hong YM, Lee H, Cho M-S, Kim KC (2017) Apoptosis and remodeling in adriamycin-induced cardiomyopathy rat model. Korean J Pediatr 60:365–372

Huang CX, Yuan MJ, Huang H, Wu G, Liu Y, Yu SB, Li HT, Wang T (2009) Ghrelin inhibits post-infarct myocardial remodeling and improves cardiac function through anti-inflammation effect. Peptides 30:2286–2291

Işeri SO, Sener G, Saglam B, Ercan F, Gedik N, Yeğen BC (2008) Ghrelin alleviates biliary obstruction-induced chronic hepatic injury in rats. Regul Pept 146(1–3):73–79

Jacoby JJ, Kalinowski A, Liu M-G, Zhang SS-M, Gao Q, Chai G-X, Ji L, Iwamoto Y, Li E, Schneider M (2003) Cardiomyocyte-restricted knockout of STAT3 results in higher sensitivity to inflammation, cardiac fibrosis, and heart failure with advanced age. Proc Natl Acad Sci U S A 100:12929–12934

Johnson TA, Singla DK (2018) PTEN inhibitor VO-OHpic attenuates inflammatory M1 macrophages and cardiac remodeling in doxorubicin-induced cardiomyopathy. Am J Physiol Heart Circ Physiol 315:H1236

Kihara M, Kaiya H, Win ZP, Kitajima Y, Nishikawa M (2016) Protective effect of dietary ghrelin-containing salmon stomach extract on mortality and cardiotoxicity in doxorubicin-induced mouse model of heart failure. J Food Sci 81:H2858–H2865

Kojima M, Hosoda H, Matsuo H, Kangawa K (2001) Ghrelin: discovery of the natural endogenous ligand for the growth hormone secretagogue receptor. Trends Endocrinol Metab 12:118–122

Kui L, Weiwei Z, Ling L, Daikun H, Guoming Z, Linuo Z, Renming H (2009) Ghrelin inhibits apoptosis induced by high glucose and sodium palmitate in adult rat cardiomyocytes through the PI3K-Akt signaling pathway. Regul Pept 155:62–69

Kumar D, Kirshenbaum LA, Li T, Danelisen I, Singal PK (2001) Apoptosis in adriamycin cardiomyopathy and its modulation by probucol. Antioxid Redox Signal 3:135–146

Kunisada K, Negoro S, Tone E, Funamoto M, Osugi T, Yamada S, Okabe M, Kishimoto T, Yamauchi-Takihara K (2000) Signal transducer and activator of transcription 3 in the heart transduces not only a hypertrophic signal but a protective signal against doxorubicin-induced cardiomyopathy. Proc Natl Acad Sci U S A 97:315–319

L'Ecuyer T, Sanjeev S, Thomas R, Novak R, Das L, Campbell W, Heide RV (2006) DNA damage is an early event in doxorubicin-induced cardiac myocyte death. Am J Physiol Heart Circ Physiol 291: H1273–H1280

Lee J, Hong F, Kwon S, Kim SS, Kim DO, Kang HS, Lee SJ, Ha J, Kim SS (2002) Activation of p38 MAPK induces cell cycle arrest via inhibition of Raf/ERK pathway during muscle differentiation. Biochem Biophys Res Commun 298:765–771

Li SP, Junttila MR, Han J, Kahari VM, Westermarck J (2003) p38 mitogen-activated protein kinase pathway suppresses cell survival by inducing dephosphorylation of mitogen-activated protein/extracellular signal-regulated kinase kinase1,2. Cancer Res 63: 3473–3477

Li Y, Hai J, Li L, Chen X, Peng H, Cao M, Zhang Q (2013) Administration of ghrelin improves inflammation, oxidative stress, and apoptosis during and after non-alcoholic fatty liver disease development. Endocrine 43:376–386

Liu M, Li Y, Liang B, Li Z, Jiang Z, Chu C, Yang J (2018) Hydrogen sulfide attenuates myocardial fibrosis in diabetic rats through the JAK/STAT signaling pathway. Int J Mol Med 41:1867–1876

Lou H, Danelisen I, Singal PK (2005) Involvement of mitogen-activated protein kinases in adriamycin-induced cardiomyopathy. Am J Physiol Heart Circ Physiol 57:H1925

Lu Z, Xu S (2006) ERK1/2 MAP kinases in cell survival and apoptosis. IUBMB Life 58:621–631

Mantawy EM, El-Bakly WM, Esmat A, Badr AM, El-Demerdash E (2014) Chrysin alleviates acute doxorubicin cardiotoxicity in rats via suppression of oxidative stress, inflammation and apoptosis. Eur J Pharmacol 728:107–118

Masson PJ (1929) Some histological methods: trichrome stainings and their preliminary technique. J Tech Methods 12:75

Mousseaux D, Le Gallic L, Ryan J, Oiry C, Gagne D, Fehrentz J-A, Galleyrand J-C, Martinez J (2009) Regulation of ERK1/2 activity by ghrelin-activated growth hormone secretagogue receptor 1A involves a PLC/PKCε pathway human GHSR-1a-mediated ERK1/2 activation. Br J Pharmacol 148:350–365

Nagaya N, Kojima M, Uematsu M, Yamagishi M, Hosoda H, Oya H, Hayashi Y, Kangawa K (2001a) Hemodynamic and hormonal effects of human ghrelin in healthy volunteers. Am J Physiol Regul Integr Comp Physiol 280:R1483–R1487

Nagaya N, Uematsu M, Kojima M, Ikeda Y, Yoshihara F, Shimizu W, Hosoda H, Hirota Y, Ishida H, Mori H, Kangawa K (2001b) Chronic administration of ghrelin improves left ventricular dysfunction and attenuates development of cardiac cachexia in rats with heart failure. Circulation 104:1430–1435

Nagaya N, Moriya J, Yasumura Y, Uematsu M, Ono F, Shimizu W, Ueno K, Kitakaze M, Miyatake K, Kangawa K (2004) Effects of ghrelin administration on left ventricular function, exercise capacity, and muscle wasting in patients with chronic heart failure. Circulation 110:3674–3679

Nanzer A, Khalaf S, Mozid A, Fowkes R, Patel M, Burrin J, Grossman A, Korbonits M (2004) Ghrelin exerts a proliferative effect on a rat pituitary somatotroph cell line via the mitogen-activated protein kinase pathway. Eur J Endocrinol 151:233–240

Negoro S, Kunisada K, Fujio Y, Funamoto M, Darville MI, Eizirik DL, Osugi T, Izumi M, Oshima Y, Nakaoka Y (2001) Activation of signal transducer and activator of transcription 3 protects cardiomyocytes from hypoxia/reoxygenation-induced oxidative stress through the upregulation of manganese superoxide dismutase. Circulation 104:979–981

Octavia Y, Tocchetti CG, Gabrielson KL, Janssens S, Crijns HJ, Moens AL (2012) Doxorubicin-induced cardiomyopathy: from molecular mechanisms to therapeutic strategies. J Mol Cell Cardiol 52:1213–1225

Pei XM, Yung BY, Yip SP, Ying M, Benzie IF, Siu PM (2013) Desacyl ghrelin prevents doxorubicin-induced myocardial fibrosis and apoptosis via the GHSR-independent pathway. Am J Physiol Endocrinol Metab 306:E311–E323

Pei XM, Yung BY, Yip SP, Chan LW, Wong CS, Ying M, Siu PM (2015) Protective effects of desacyl ghrelin on diabetic cardiomyopathy. Acta Diabetol 52:293–306

Pipicz M, Demján V, Sárközy M, Csont T (2018) Effects of cardiovascular risk factors on cardiac STAT3. Int J Mol Sci 19:3572

Podewski EK, Hilfiker-Kleiner D, Hilfiker A, Morawietz H, Lichtenberg A, Wollert KC, Drexler H (2003) Alterations in Janus kinase (JAK)-signal transducers and activators of transcription (STAT) signaling in patients with end-stage dilated cardiomyopathy. Circulation 107: 798–802

Poizat C, Puri PL, Bai Y, Kedes L (2005) Phosphorylation-dependent degradation of p300 by doxorubicin-activated p38 mitogen-activated protein kinase in cardiac cells. Mol Cell Biol 25:2673–2687

Riad A, Bien S, Westermann D, Becher PM, Loya K, Landmesser U, Kroemer HK, Schultheiss HP, Tschöpe C (2009) Pretreatment with statin attenuates the cardiotoxicity of doxorubicin in mice. Cancer Res 69:695–699

Rossi F, Castelli A, Bianco MJ, Bertone C, Brama M, Santiemma V (2009) Ghrelin inhibits contraction and proliferation of human aortic smooth muscle cells by cAMP/PKA pathway activation. Atherosclerosis 203:97–104

Sauter KAD, Wood LJ, Wong J, Iordanov M, Magun BE (2011) Doxorubicin and daunorubicin induce processing and release of interleukin-1 beta through activation of the NLRP3 inflammasome. Cancer Biol Ther 11:1008–1016

Scarabelli TM, Mariotto S, Abdel-Azeim S, Shoji K, Darra E, Stephanou A, Chen-Scarabelli C, Marechal JD, Knight R, Ciampa A (2009) Targeting STAT1 by myricetin and delphinidin provides efficient protection of the heart from ischemia/reperfusion-induced injury. FEBS Lett 583:531–541

Shizukuda Y, Matoba S, Mian OY, Nguyen T, Hwang PM (2005) Targeted disruption of p53 attenuates doxorubicin-induced cardiac toxicity in mice. Mol Cell Biochem 273:25–32

Stephanou A, Brar BK, Scarabelli TM, Jonassen AK, Yellon DM, Marber MS, Knight RA, Latchman DS (2000) Ischemia-induced STAT-1 expression and activation play a critical role in cardiomyocyte apoptosis. J Biol Chem 275:10002–10008

Wallace KB (2003) Doxorubicin-induced cardiac mitochondrionopathy. Pharmacol Toxicol 93:105–115

Wang X, Shaw S, Amiri F, Eaton DC, Marrero MB (2002) Inhibition of the Jak/STAT signaling pathway prevents the high glucose-induced increase in TGF-β and fibronectin synthesis in mesangial cells. Diabetes 51:3505–3509

Wang X, Wang X-L, Chen H-L, Wu D, Chen J-X, Wang X-X, Li R-L, He J-H, Mo L, Cen X, Wei Y-Q, Jiang W (2014) Ghrelin inhibits doxorubicin cardiotoxicity by inhibiting excessive autophagy through AMPK and p38-MAPK. Biochem Pharmacol 88:334–350

Wu Z, Li W, Sun Y, Fu K, Cheng S (2017) Eleutheroside E inhibits doxorubicin-induced inflammation and apoptosis in rat cardiomyocytes by modulating activation of NF-κB pathway. Trop J Pharm Res 16:515–523

Xiang Y, Li Q, Li M, Wang W, Cui C, Zhang J (2011) Ghrelin inhibits AGEs induced apoptosis in human endothelial cells involving ERK1/2 and PI3K/Akt pathways. Cell Biochem Funct 29:149–155

Xu Z, Wu W, Zhang X, Liu G (2007) Endogenous ghrelin increases in adriamycin-induced heart failure rats. J Endocrinol Investig 30:117–125

Xu Z, Lin S, Wu W, Tan H, Wang Z, Cheng C, Lu L, Zhang X (2008) Ghrelin prevents doxorubicin-induced cardiotoxicity through TNF-alpha/NF-κB pathways and mitochondrial protective mechanisms. Toxicology 247:133–138

Yang C, Liu Z, Liu K, Yang P (2014) Mechanisms of ghrelin antiheart failure: inhibition of Ang II induced cardiomyocyte apoptosis by down-regulating AT1R expression. PLoS One 9:e85785

Zhang G, Yin X, Qi Y, Pendyala L, Chen J, Hou D, Tang C (2010) Ghrelin and cardiovascular diseases. Curr Cardiol Rev 6:62–70